Acoustic emission wave propagation in pipeline sections and analysis of the effect of coating and sensor location.

RAJENDRAN, V., PRATHURU, A., FERNANDEZ, C. and FAISAL, N.

2024

Nondestructive Testing and Evaluation

ISSN: (Print) (Online) Journal homepage: www.tandfonline.com/journals/gnte20

Acoustic emission wave propagation in pipeline sections and analysis of the effect of coating and sensor location

Vinooth Rajendran, Anil Prathuru, Carlos Fernandez & Nadimul Faisal

To cite this article: Vinooth Rajendran, Anil Prathuru, Carlos Fernandez & Nadimul Faisal (20 Aug 2024): Acoustic emission wave propagation in pipeline sections and analysis of the effect of coating and sensor location, Nondestructive Testing and Evaluation, DOI: 10.1080/10589759.2024.2390996

To link to this article: https://doi.org/10.1080/10589759.2024.2390996

Published online: 20 Aug 2024.

NONDESTRUCTIVE TESTING AND EVALUATION
https://doi.org/10.1080/10589759.2024.2390996

Taylor & Francis
Taylor & Francis Group

Acoustic emission wave propagation in pipeline sections and analysis of the effect of coating and sensor location

Vinooth Rajendran[a], Anil Prathuru[a], Carlos Fernandez[b] and Nadimul Faisal[a]

[a]School of Engineering, Robert Gordon University, Aberdeen, UK; [b]School of Pharmacy and Life Sciences, Robert Gordon University, Aberdeen, UK

ABSTRACT

This paper presents an experimental investigation in which acoustic emission (AE) wave was generated through a pencil lead break as a point source on two pipeline sections made of mild steel and titanium. The pipelines (bare, epoxy phenolic coated) were of same length but had two different diameters and wall thicknesses. The recorded AE signals were analysed using time and frequency domain signals, energy levels and wavelet transform to explore time-frequency features for the identification of wave modes. It is concluded that the damping behaviour of coating restricts the peaks of waves, decreases the decay time of waves and reduces the energy level in the coated pipeline. It is concluded that monitoring of coated pipeline wave propagation could be done effectively with sensor placement directly on the pipeline surface compared to sensor placement on the coating surface. A high wall thickness of pipeline results in a higher number of reflected waves and increases the decay time of waves. The coating on pipeline resists wave propagation, and different densities of coating layer and pipeline affect the velocity of the wave. This experimental work advance towards designing an alternative way to monitor changes in pipeline structures (e.g., corrosion under insulation applications).

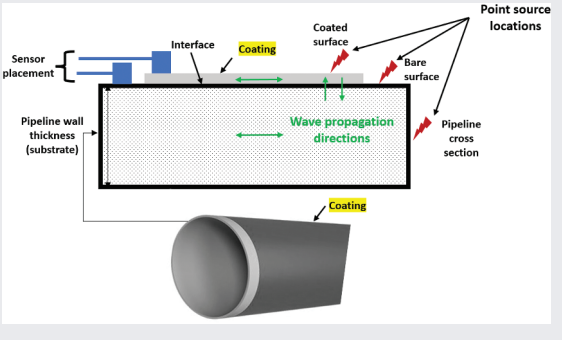

ARTICLE HISTORY
Received 13 February 2024
Accepted 6 August 2024

KEYWORDS
Acoustic emission; pipeline; pencil lead break; epoxy phenolic coating; wavelet transform; sensor location

CONTACT Nadimul Faisal N.H.Faisal@rgu.ac.uk

1. Introduction

Metal pipelines can be subjected to variety of defects such as corrosion, cracking, pitting, creep, fatigue and weld defects. Protecting bare pipeline through cost effective coating is among the most reliable corrosion prevention methods. Additionally, applying insulation to pipelines (whether bare or coated) or rubber sheet is a common practice for various reasons, including managing hot or cold temperatures, controlling sound and vibrations and optimising process efficiency. In such cases, such as the deposition of coating or insulation or a combination of both on pipelines, interfaces are introduced. Among these interface conditions, corrosion under insulation (CUI) is a commonly used term, representing a form of localised corrosion affecting various industries and sectors. The moisture penetration and storage at the interface conditions accelerate corrosion. Corrosion at the interface poses significant challenges for many industries, including high maintenance costs (accounting for around 40% to 60% of total equipment maintenance) and a system failure that often remains undetected until failure occurs [1]. Chemical, electrochemical and other reactions occurring at the interface, which are largely hidden visually, retain reactants at the interface region, increasing continuous materials degradation and leading to system failure. To prevent these failures, AE sensors offer a potential way to monitor changes at the interface. Addressing these issues at a fundamental level involves understanding the effect of coating on pipelines, making the use of sensing methods crucial in this subject area with some advancements.

Insulated, coated or non-coated pipeline conditions can be detected through traditional inspection methods such as ultrasonic thickness measurement, profile radiography, neutron backscatter, infrared thermography and pulsed eddy current testing (PECT). As an example, PECT method induces eddy currents, and the probe measures wall thickness by tracking the time taken by the eddy currents to decay. The thicker the wall, the longer it takes for the eddy currents to decay to zero. PECT method is also used to detect inner wall flaws and other conditions in pipe based on pulsed eddy current [2,3]; however, such method can only be used on conductive materials. Inspection is essential to provide safe operating conditions and prevent environmental impacts. Inspection methods selection is based on the size and condition of the pipeline, environmental situations and economic value [4]. Each inspection method has its limitations, such as the expensive process for large pipeline sections, requiring another method to quantify the corrosion and corrosion type, and some radiography methods causing human health issues with a lack of safety measures. The disadvantage of inspection methods is that they do not provide continuous information about the pipeline conditions. If inspections are carried out very frequently, in that case, the maintenance cost increases, and sometimes the plant needs to shut down completely to carry out the inspection, which leads to a loss of production. An alternative way of sensing is required to monitor the changes on pipeline under coating and insulation, which could then help provide precise details of the interface(s) conditions. As previous studies suggested that acoustic emission (AE) sensors could monitor structural health of complex structures in different conditions. However, the effect of coating (epoxy phenolic) and sensor locations are undiscovered. Through this research and as part of preliminary step, the aim is to experimentally investigate AE wave transmission generated through a point source conducted on various pipeline sections (i.e. varying the directionality) and differentiate the wave propagation (and identify the effects of coatings, pipeline materials, pipe wall thicknesses and sensor locations).

AE method has been used in various interface monitoring applications, such as CUI and reinforced concrete steel, to monitor interface corrosion. Due to release of strain energy, AE waves mainly emerge from corrosion and cracking of the pipeline's surface and secondly rise from peeling off and removing corrosion products from corroded areas [5,6]. AE sensor monitoring can also be one of the effective methods with high sensitivity. It is used in various applications such as monitoring the pipeline, storage tanks and pressure vessels to prevent leakages and monitor metal fatigue, stress and partial deformation on the metal surface. Shehadeh, Steel and Reuben [7] proposed a method to detect the source location on the pipeline surface based on the wave's arrival time. AE waves reaching the sensor depend on the distance between sensor and source location and geometry of the pipeline. AE sensor away from the source location receives reduced amplitude, frequency and energy level with a high level of dispersion. AE reflected and transmitted wave behaviour depends on the pipeline properties [8]. Waves propagation depends on the material's properties and structure. Since the pipeline is cylindrical, and due to such geometry, AE waves propagate around the pipeline surface [9]. The high thickness with low pipeline density provides enough space for the wave's propagation for a long time, resulting in a higher amplitude of the waves. Additionally, the wave velocity is inversely proportional to the density and directly proportional to the elastic modulus of the pipeline. The high-density pipeline restricts the wave's propagation time, speed and energy [8,10].

Other researchers have used AE sensors to study the propagation of AE waves in pipeline-like structure. Specialised AE sensors (e.g. low-frequency sensors) can be used to monitor corrosion at the interface of storage tanks due to low noise levels in such storage facilities [6,11]. Cho, Tamura and Matsuo [5] used AE sensors and monitored signals from CUI using two small AE sensors attached near the two ends of the insulation section. AE was measured under two different conditions, i.e. humidification and dry. From analysis, it was observed that most AE signals were detected during the drying process in each wetting and drying cycle when the humidity was more than 95% relative humidity, with sources located around corrosion region. It was also observed that AE rate increased with the time of wetness or the period of humidification.

Considering leak in pipeline as a localised AE source in a pipeline, using cross-correlation function, Ozevin and Harding's [9] approach was to determine arrival time differences and introduce the geometric connectivity to identify the path that the leak waves should propagate to reach the AE sensors. It was demonstrated that the two-dimensional location of a leak in a pipeline network could be determined using the one-dimensional source location algorithm integrated with geometric connectivity. Mostafapour and Davoudi [12] analysed leakage in high-pressure pipe using AE method and modelled pipeline vibration caused by AE generated due to escaping of fluid, and the results indicated the good agreement between the experimental and modelled frequencies ranges. Xu et al. [13] proposed a method to locate the leakage source in pipelines with a single AE sensor. It was suggested that such method could help obtain precise localisation for a longer source-to-sensor distance. Considering a combination of frequency matching, dispersive properties and modes confusing possibilities, a criterion was presented to select the suitable wave modes for leakage localisation. Also, using the wavelet transform (WT) approach, the arrival time difference between specific wave modes was calculated, and the corresponding group velocities for specific modes were

then obtained per the frequencies that maximise the WT magnitudes. It was suggested that the source-to-sensor distance could be calculated with the known arrival time difference and group velocities.

Barat et al. [14] developed analytical model of AE signals in thin-walled objects and based on the modal analysis of Lamb wave propagation developed the algorithm for AE impulse waveform simulation. Based on the results it was concluded that the modal analysis of the normal waves propagation, supplemented by an analytical calculation of Lamb wave attenuation, can be an effective analytical method for calculating the propagation of AE signals along a waveguide. A full description of Lamb wave theory can be found by Su and Ye [15]. Recently, Mahmoud et al. [16] demonstrated the AE wave relationship with differently loaded pneumatic cylinders. It was shown that the progress and retreat stroke change with the position of the load and the damaged and undamaged cylinder conditions. It was also suggested that the leaks can be detected and located as long as the pressure fluid acts across the leak. Jones et al. [17] established a novel approach to locating AE sources in complex structures using a Bayesian methodology, which can offer finding multiple damage locations and mapping the area for inspection.

Through some recent research, it has been demonstrated that the AE method can be useful for assessing the condition of gas pipelines made of steel material. Example included tests to identify the damage process in steel pipeline subjected to quasi-static loading-uniaxial tension until failure [18], assessing the effect of the introduction of a sharp V-shaped notch on the failure process of a uniaxially tensile specimens [19,20] and then establishing relationships between characteristic types of AE signals and pipeline material destruction processes. Overall, it was shown that the AE signals are valuable in developing a quality-driven methodology for monitoring the operational safety of gas network pipelines.

Various studies have discussed wave propagation in pipelines under different test conditions. However, this experimental study was carried out with the aim to understand the effect of coating on wave propagation and monitoring changes based on the sensor placement conditions. These findings will be directly helpful in designing sensor-based monitoring systems for various degradation and monitoring of pipeline-like structures. Furthermore, understanding of the wave behaviour based on the coated pipeline and coating removal (CR) at sensor location conditions can lead to advancements in corrosion detection and prevention techniques. This paper presents an experimental investigation where AE was generated through a pencil lead break (PLB) as point source conducted on various pipeline points of same length (bare and coated pipelines of mild steel and titanium) to identify the effects of coatings, pipeline materials (density), pipe wall thicknesses and wave propagation directionality. Time domain, frequency domain, AE parameters, WT and AE energy level analysis methods have been used to understand wave propagation characteristics.

2. Methodology

This section includes details about experimental conditions and analysis methodologies to investigate the influence of coating layer, materials properties, wall thickness and significant of sensor location on AE propagation through the bare and coated pipelines made of mild steel and titanium. PLB tests were conducted to simulate AE point sources

on bare and coated pipelines at various points. Epoxy phenolic coating was used in this investigation, as such coating is among the most used ones in CUI application and preventing corrosion at the interface.

2.1. AE instrumentation

A customised AE instrument was assembled which included an AE sensor, preamplifier and multipurpose data acquisition (DAQ) card to monitor AE waves in a cost-effective way. Cylindrical shaped Micro-80D sensors (diameter: 0.375 mm, height: 10 mm) are from Physical Acoustics Corporation (PAC) based on lead zirconate titanate (PZT) with a frequency response range of 100–900 kHz with peak response at 320 kHz. The AE instrument block diagram is shown in Figure 1. The preamplifiers were used to amplify the signals. The Mistras group preamplifier (PAC series 1220A) has three levels of amplification: 20 dB, 40 dB and 60 dB. The sensor was connected to a differential input point, and the generated voltage signals pass through the power signal cable to the signal processing unit. A suitable amplification was chosen for each case to suit the detectable range of the data acquisition unit.

The signal processing unit has a four-channel system that was coupled with a gain-programmer to provide a 28 V power-supply, coupled with adjustable amplification levels of −12 dB, 0 dB, +6 dB and +12 dB gain control [21]. In this experiment, the preamplifier gain was set at 60 dB, signal processing unit gain was +12 dB and the number of data points per record and sampling rate was 100,000 and 2,500,000 samples/s, respectively. The National Instruments BNC 2110 connects the signal processing unit to the multipurpose data acquisition card (NI 6115). It can record the signals on four channels (each channel recording at 2.5 MS/s (million samples per second)). A virtual interface using LabVIEW code provided selection options of several channels, a number of scans, sampling rate, trigger channel, pre-trigger scans, pre-trigger level and file storage location. The trigger level was kept at 0.2 to avoid natural and other sound interruptions. The sample frequency (sampling rate) had to be chosen to be at least double of the maximum expected signal frequency to ensure accurate capture of the signal data without losing information.

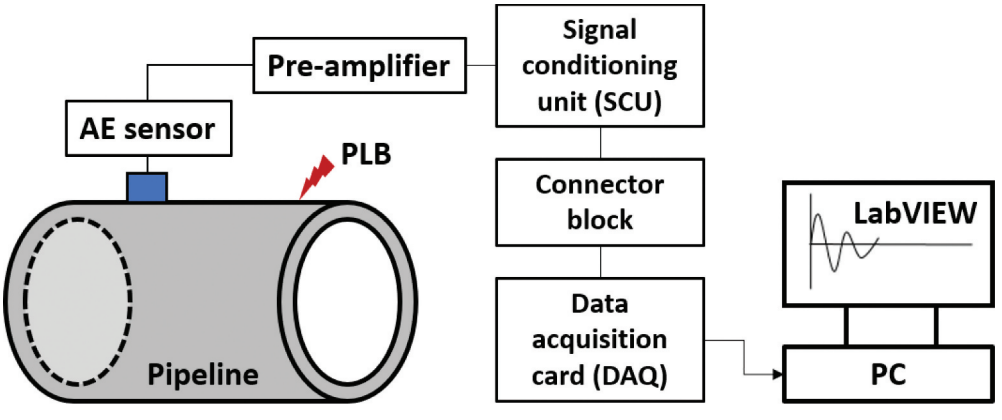

Figure 1. Block diagram of the AE instrument used for the investigation.

2.2. PLB tests

The PLB test has been widely used as a point source for test signals in AE applications, which is also called the Hsu-Nielsen source, based on the original works of Hsu and Nielsen (ASTM E 976-99 Standard)22. The pencil lead is pressed on the surface of the structure in the PLB test until the lead breaks. Pressing the lead on the surface puts pressure on the material locally. When the lead breaks, the accumulated stress is released suddenly, inducing a microscopic displacement of the surface and consequently acoustic wave propagation in the structure.

The advantage of this method is that it can be easily handled in laboratory environments and field testing, making it a prevalent method of simulating AE point source in structural integrity testing. The lead (pencil) diameter, lead length and angle of lead breaking can induce variations in the generated acoustic waves. For the repeatability of the test, it is recommended to use the same angle, diameter and lead length. The properties of the lead are usually 0.3- or 0.5-mm diameter, 2 H hardness, the breaking angle is between 20° and 60° and the length of the lead is typically 2–3 mm. The PLB source frequency range is 40–600 kHz [23,24]. In this experimental work, the AE point source was generated by breaking lead pencil close and away from the sensor, at the inner and cross-section locations of the pipeline (shown in Figure 2) for the two pipelines with two different conditions (i.e. bare, coated). It is important to note that elastic wave from PLB test is very much sensitive to the angle of pencil, length of the lead and strength applied on the lead until break. To ensure the quality of experimental results, the PLB test was carried out at each point five times. The distance between sensor and PLB test points remained consistent in all experimental conditions, and the results are plotted along with standard deviations to illustrate the range.

2.3. Pipeline samples and experimental setup

The experimental approach involving investigating AE wave propagation in the pipeline. Pipeline and coating properties are as follows: mild steel (elastic modulus: 190–210 GPa, Poisson's ratio: 0.27–0.30, density: 7800–8000 kg/m^3) [25]; titanium alloy (elastic modulus: 115 GPa, Poisson's ratio: 0.35, density: 4430 kg/m^3) [26–28]; epoxy phenolic coating (elastic modulus: 2.7–4.1 GPa, Poisson's ratio: 0.31, density: 1200–1400 kg/m^3) [29,30]. The pipeline sample details, and the experimental matrix is presented in Table 1. To investigate AE wave propagation in the pipeline, two different pipeline materials of different densities (mild steel, titanium) were selected to understand the effect and lack thereof coatings and assess the significance of sensor locations. As stated above, the titanium alloy has a lower density compared to the mild steel. Using the PLB test, the AE waves propagation and parameters were investigated on three types (i.e. bare, coated and CR at sensor locations) of pipeline samples, as shown schematically in Figure 2. Some experimental pipeline (original) samples are shown in Figure 3. Epoxy phenolic coating layers on the outer surface were brush painted on both bare pipeline sections (mild steel, i.e., (ASTM A106) or seamless pressure pipe (also known as ASME SA106 pipe), and titanium).

The AE sensor 1 (S1) was placed at location O; AE sensor 2 (S2) was placed at location Q in all conditions of PLB tests on two pipelines. The sensors' sensitive area (bottom

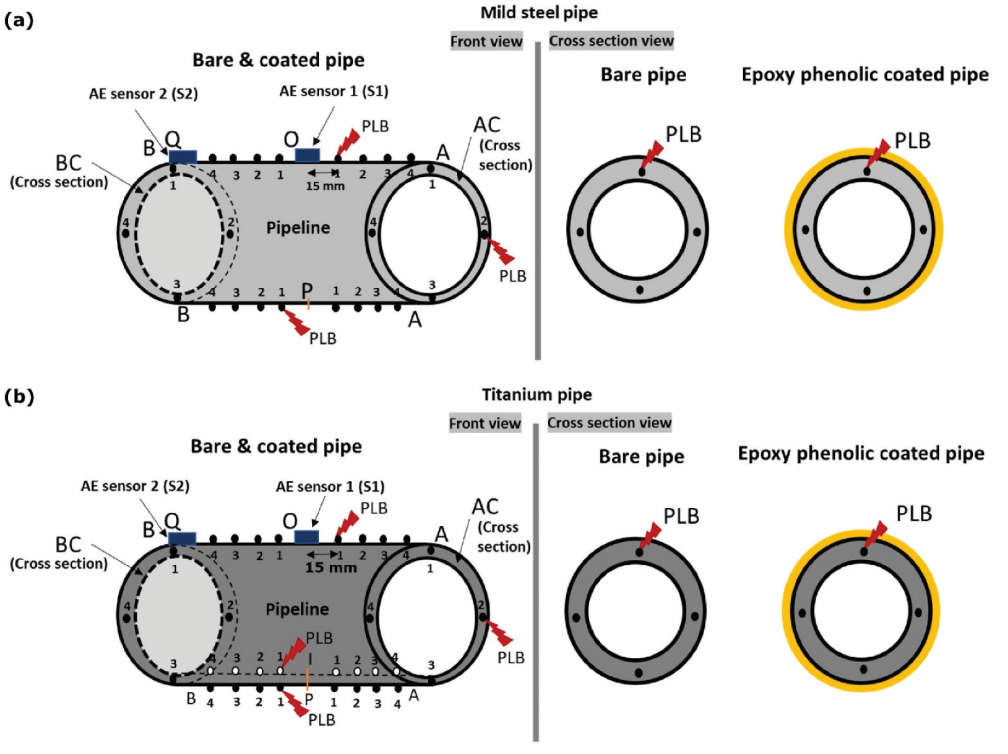

Figure 2. PLB test points, directionality and AE sensor locations in two pipeline sections: (a) mild steel and (b) titanium.

area) was in complete contact with the pipelines, as shown in Figure 2 sensors placements. To obtain good transmission of the AE signal, the surface was kept smooth and clean, and silicone high vacuum grease was used as coupling layer to fill any gaps caused by roughness of the surface and to eliminate air which might otherwise impair wave transmission [31]. AE point source was generated by breaking lead pencil close and away from the sensors, at the inner and cross-section locations of the pipeline for the two pipelines with three different conditions: (a) PLB test on the outer pipeline surface close to the sensor (OA, OB direction), (b) PLB test on the outer pipeline surface away (opposite side) from the sensor (PA, PB direction), (c) PLB test on the cross-section of the pipeline (AC, BC side), (d) PLB test on inner surface of the pipeline (IA, IB direction) (Figure 2). The PLB test was not carried along the inner circumference for smaller diameter (60 mm) mild steel pipeline sections due to limited access to inner locations. PLB test was carried out in various conditions such as OA and OB (close to the sensor), each side with four points with a distance between the points of 15 mm. PA, PB (away from the sensor) each side four points with 15 mm distance. Four points on AC and BC sides with a 90° angle on each side. IA and IB (inner surface) each side four points with 15 mm distance (Figure 2). At each PLB locations, five PLBs were performed, and the results are presented with the standard deviations to see the range of AE energy.

The AE experiment started with bare mild steel (with 60 mm outer diameter) and titanium (with 166 mm outer diameter) pipelines as shown in Figure 3(a,d). The epoxy

Table 1. Pipeline sample details and experimental matrix.

Sr. no.	Pipeline materials	Length (mm)	Outer diameter (mm)	Pipeline thickness (mm)	Bare and coating material deployed		PLB points (at each location, five PLB tests were carried)	PLB direction (directionality)
1	Mild steel (MS)	155	60	5	Bare pipe	Epoxy phenolic coating (0.272 mm thick, with tandard deviation of 0.012)	1, 2, 3, 4	OA, OB, PA, PB, AC, BC
2	Titanium alloy (Ti)	155	166	18	Bare pipe	Epoxy phenolic coating (0.306 mm thick, with standard deviation of 0.012)	1, 2, 3, 4	OA, OB, PA, PB, IA, IB, AC, BC

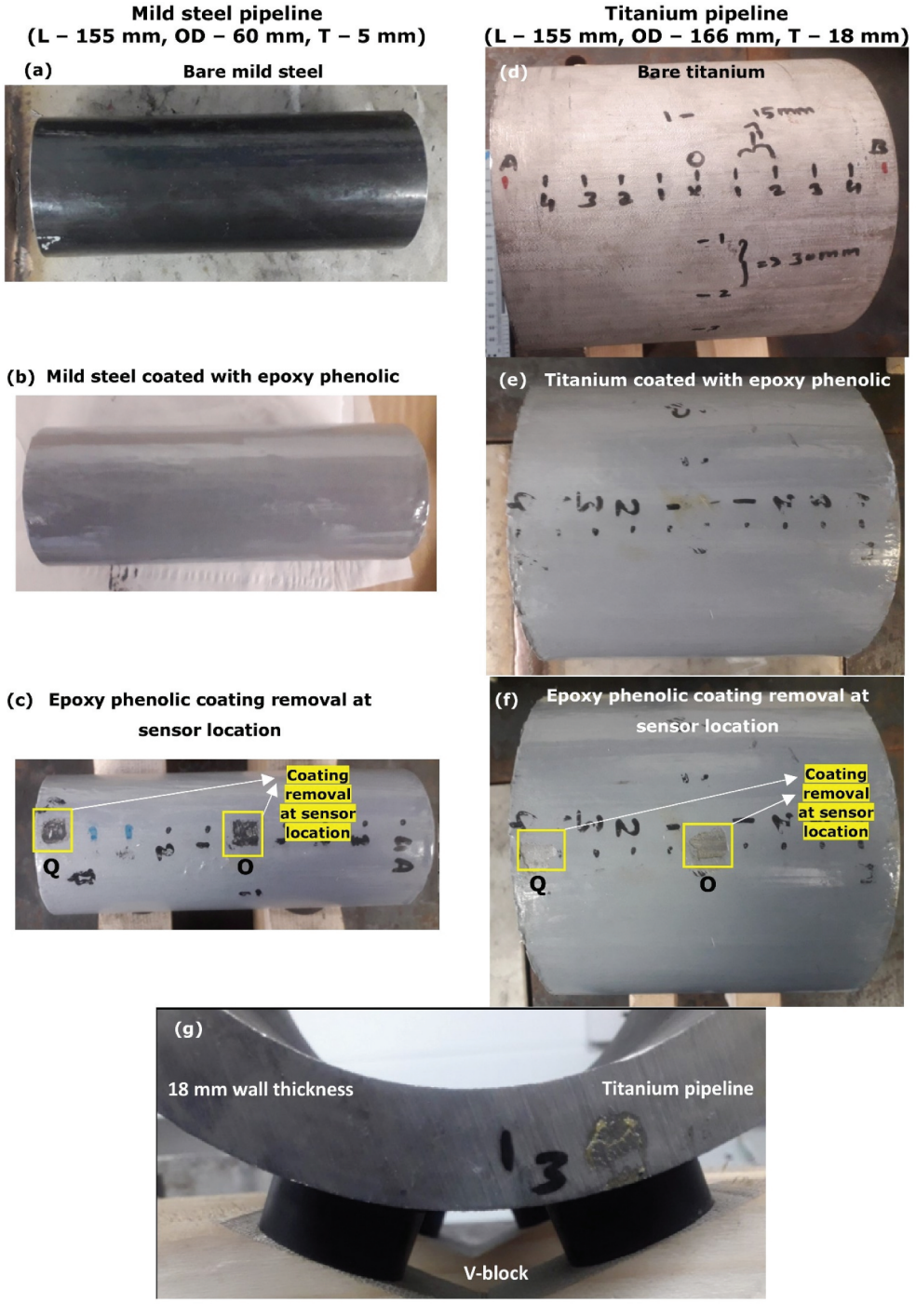

Figure 3. Pipelines: (a) bare mild steel, (b) epoxy phenolic coated mild steel, (c) coating removal at sensor location, (d) bare titanium, (e) epoxy phenolic-coated titanium, (f) coating removal at sensor locations and (g) rubber padding at the bottom of titanium pipeline with V-block support (side view).

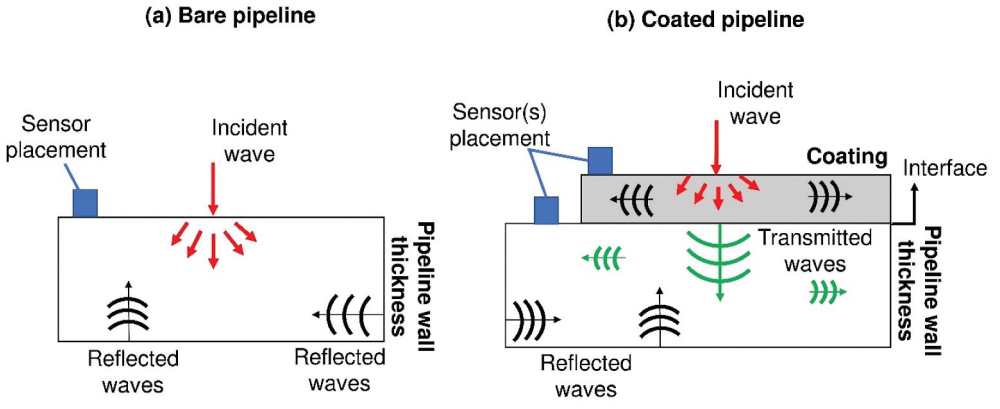

Figure 4. Schemes of incident wave location, directionality, wave propagation and sensor placement: (a) incident wave on pipeline and (b) incident wave on coating.

phenolic coating is an appropriate protective coating for the CUI purpose in industrial applications [32]. The mild steel and titanium pipeline's surface was prepared for coating with the removal of oil, grease and other unwanted elements by using sandpaper (P240, P800 and P1200). Epoxy phenolic coating and hardener were mixed in a ratio of 4:1, applied as first coating layer on the mild steel and titanium pipelines and cured for 24 h at room temperature without any external heat. The second layer of the coating was coated on both pipelines using same mixing ratio and were cured for another 24 h at room temperature without any external heat.

Epoxy phenolic coated mild steel and titanium pipelines are shown in Figure 3(b,e). The thickness of the bare and coated pipeline was measured in three locations, and the average thickness of the epoxy phenolic coating was 0.272 mm on the mild steel pipeline and 0.306 mm on the titanium pipeline. The epoxy phenolic coating was removed on the two sensor locations (O, Q) by hand tool (hammer and chisel) to mount the sensors directly on the pipeline surface. The CR at the sensor locations are shown in Figure 3(c,f). In all experimental conditions, the pipeline section was placed on a wooden support (V-block) with rubber paddings (Figure 3(g)) to isolate the pipeline and to avoid unwanted reflections at the point of contact.

2.4. Signal processing and analysis

Signal processing and analysis of wave is a complex process as it is needed to understand each wave mode's arrival time and frequency [33]. The waves can be classified into three types on a coating-pipeline wall (or substrate) section: (a) incident, (b) transmitted and (c) reflected waves, as shown in Figure 4.

The wave velocity depends on the medium of the wave's propagation and whether incident wave is on coating, or the pipeline. Guided waves that propagate along an elongated structure while guided by its boundaries, allow the waves to travel a long distance with little loss in energy and are commonly used in the structural health monitoring of pipelines to detect crack, corrosion and other

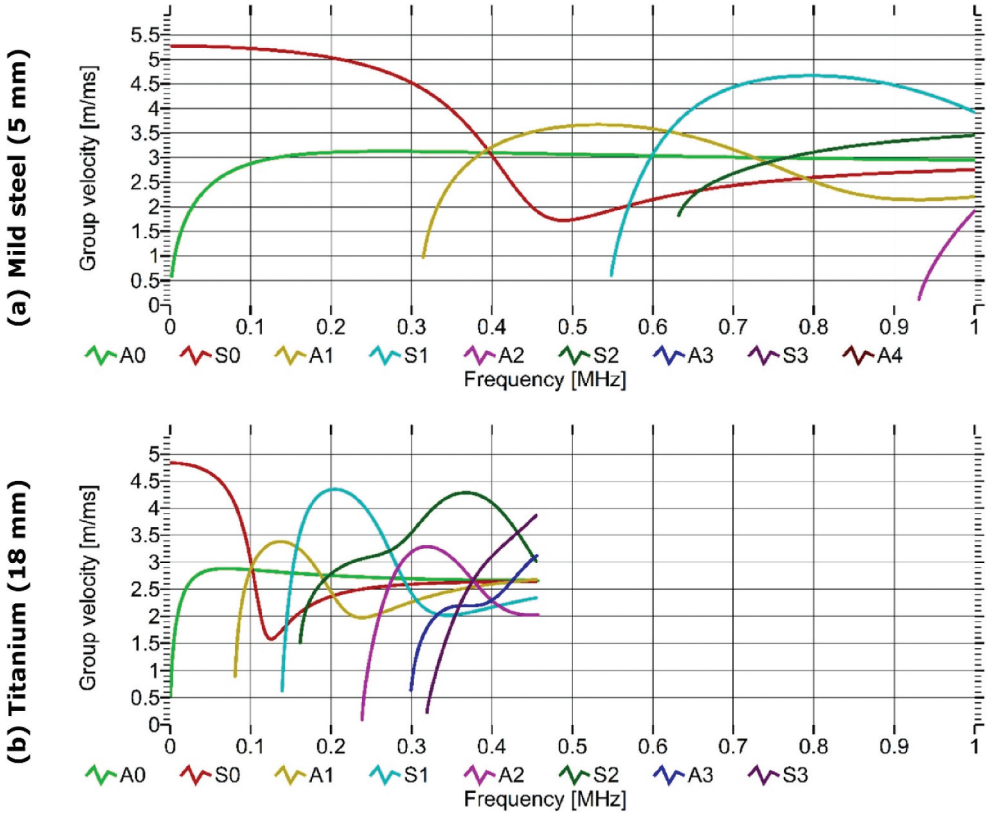

Figure 5. Dispersion curves (group velocity vs. excitation frequency) for all possible modes between 0.0 and 1.0 MHz: (a) mild steel (5 mm wall thickness) and (b) titanium (18 mm wall thickness).

failures. Pipeline guide wave propagation exhibited different wave modes, including symmetric (S0) and antisymmetric (A0) modes [34]. The symmetric mode is often called an extensional or longitudinal mode, and the antisymmetric mode is called the flexural or transverse mode [35]. The wave modes are independent of each other and propagate at different velocities. The velocity of symmetric mode is higher than antisymmetric mode within the frequency range (i.e. up to 400 kHz for mild steel (5 mm wall thickness)) [21]. Because of the different velocity propagation behaviour, the waves take different times to cover the distance from a source location to the sensor. An infinite number of modes could exist (for specific plate thickness and wave frequency), which are identified by their respective phase velocities. Waveforms overlap due to reflections from each corner and between modes. Traditionally, wave propagation characteristics are described using two dispersion curves (i.e. phase velocity (C_p) excitation frequency, or group velocity (C_g) vs. excitation frequency) (note: dispersion means change in wave speed in a material with respect to excitation frequency, whereas attenuation is the change in travelling wave amplitude over a given distance). Dispersion curves are based on the plate mode phase velocity as a function of the product

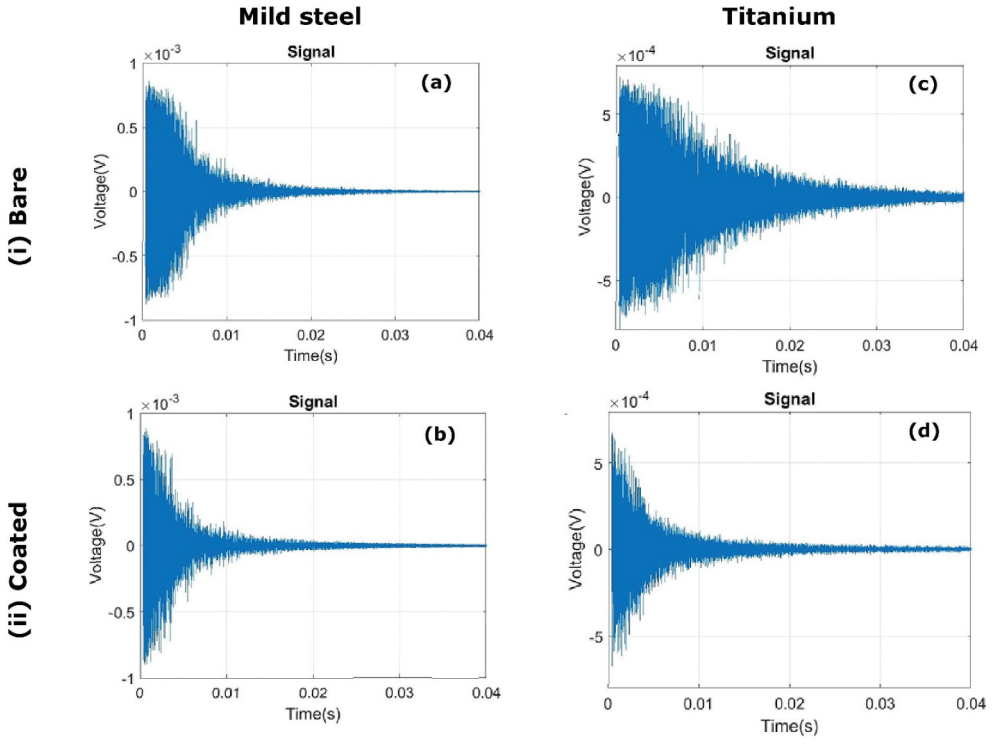

Figure 6. Representative examples of time-domain signals on pipelines: mild steel: (a) bare and (b) coated (0.272 mm thick layer); titanium: (c) bare and and (d) coated (0.306 mm thick layer) (note: time-domain signals shown here are collected from sensor 1 with PLB along OA direction at point 1).

of frequency times thickness of the plate. The dispersion curves are generally labelled as S0, A0, S1, A1, S2, A2, S3, A3, etc., depending on whether the wave mode is symmetric or antisymmetric [36].

Dispersion curves or plots of group velocity vs. frequency was generated using an open access software (AGU vallen wavelet) (R2021.1122) with 5900 m/s and 3100 m/s for longitudinal and shear waves of steel and with 5354 m/s and 2862 m/s for longitudinal and shear waves of titanium, respectively (using software's pre-set values). As shown in Figure 5, dispersion curves were generated (for mild steel pipeline of 5 mm thickness, titanium alloy pipeline of 18 mm thickness) to identify the possible modes of guided waves and its propagation characteristics in the pipeline. For mild steel pipeline thickness, zero order symmetric (S0) and antisymmetric (A0) wave modes and up to first-order antisymmetric modes (A1) existed under 400 kHz. For titanium pipeline thickness, up to third order symmetric and antisymmetric wave modes existed under 400 kHz. To simplify the wave analysis, the high-order modes waves were neglected. The group velocity of the two modes at low frequencies were significantly different, and the velocity of the symmetric mode was higher than the anti-symmetric mode in the same frequency range, which is shown in Figure 5 (Note: considering other inspection methods, the guided wave method from single-point access could certainly have advantage as the wave propagation over long distances

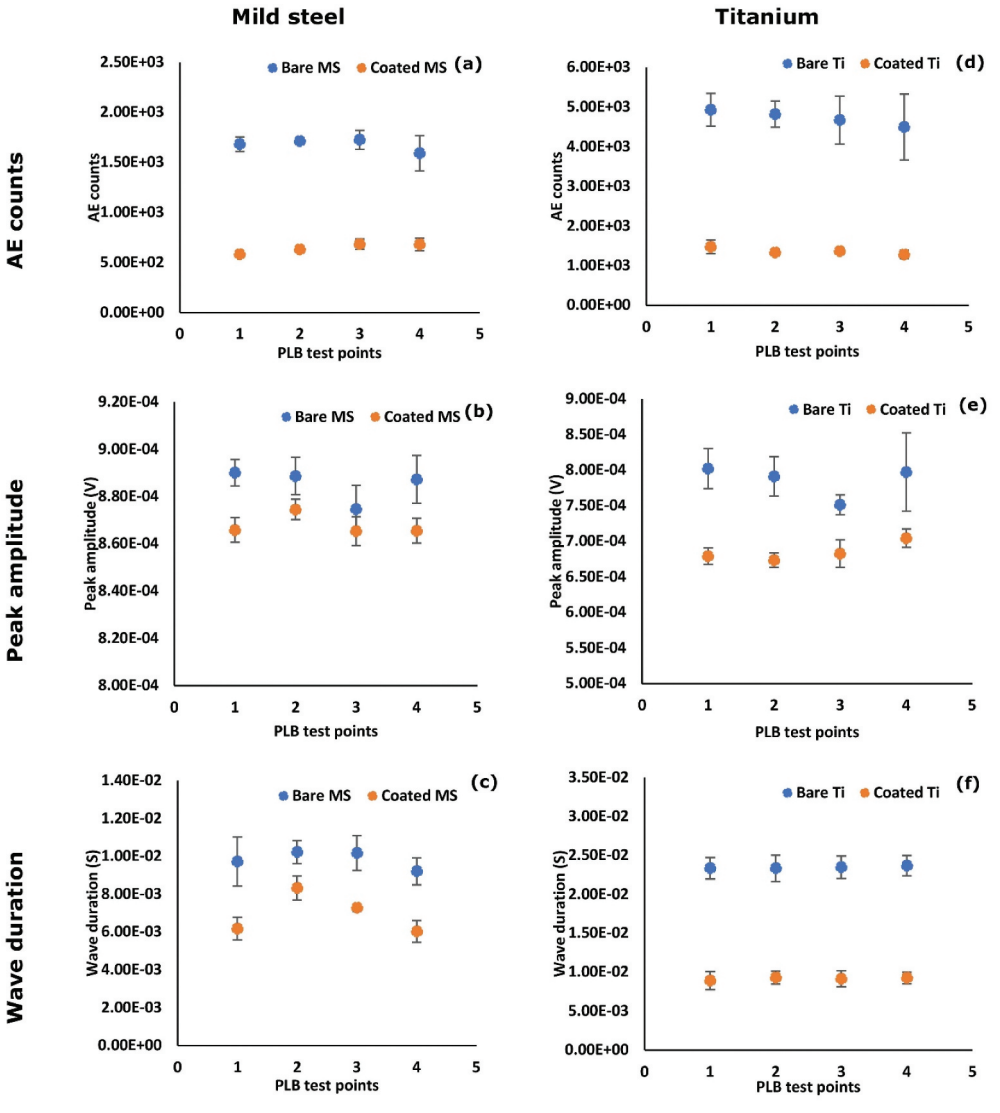

Figure 7. AE parameters comparison. Mild steel: (a) AE counts, (b) peak amplitude and (c) wave duration; titanium: (d) AE counts, (e) peak amplitude and (f) wave duration.

could allow a considerable length to be examined from a single point test locations, providing significant coverage of the sample cross-sectional area; however, such method has its own complexity [34]).

WT of time-frequency analysis is an important analysis method along with the combination of the time and frequency domains to determine the predominant frequency span along with the amplitude and time variations. It describes the time domain corresponding with frequency domain. Applying a larger frequency window at lower frequency levels, and a smaller frequency window at high frequencies confirms the excellent frequency resolution in the low-frequency range and good time resolution at high frequency. The quality is lost by applying the fixed

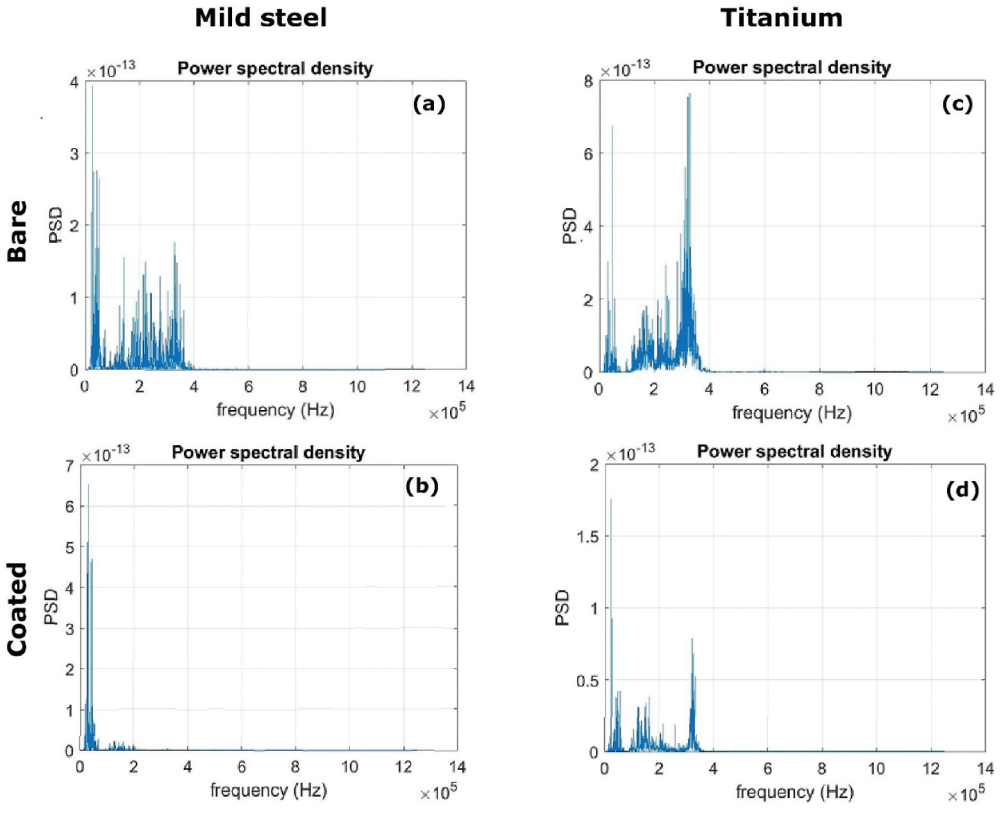

Figure 8. Representative examples of frequency domain signals of pipelines: mild steel: (a) bare and (b) coated; titanium: (c) bare and (d) coated.

frequency window [21]. MATLAB software (R2021a) was used for the energy, time and frequency domain analysis, including AE parameter analysis. The AE parameters such as wave duration, peak amplitude and counts were collected from the recorded signals with reference to the threshold values. The threshold value for each PLB test was determined by multiplying 0.2 with the maximum peak amplitude. AE signal energy (E) was calculated using $E = \int_0^t V^2(t)dt$, which is the integral of the square of the signal over the entire record [37], where V is voltage and t is time.

3. Results and discussion

This section contains two subsections. The first subsection presents results related to wave propagation in bare and coated pipeline and compares the relationship between effect of pipeline material, coating in wave propagation and parameters. The second subsection presents the effect of sensor location, comparing results between coated pipelines and those with CR at sensor locations. The overall discussion provides an understanding about AE wave propagation in bare and coated pipelines, and the significance of sensor location.

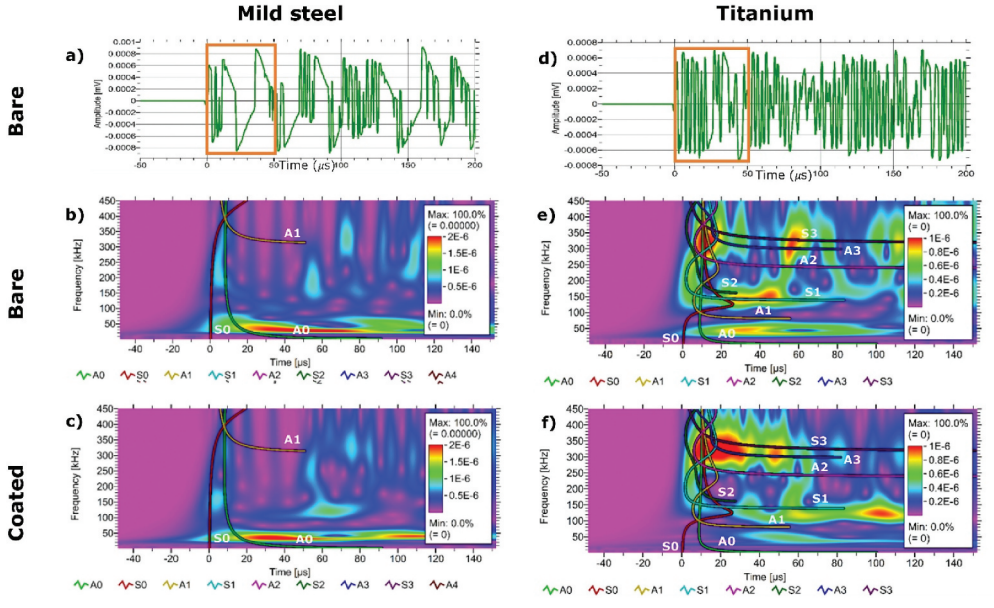

Figure 9. Representative examples of wave patterns on pipelines: mild steel: (a) wave pattern (bare mild steel), (b) WT (bare mild steel) and (c) WT (coated mild steel); titanium: (d) wave pattern (bare titanium), (e) WT (bare titanium) and (f) WT (coated titanium).

3.1. Analysis of the effect of coating

As shown in Figure 6, the time-domain analysis provides information about wave propagation on bare and coated conditions with respect to time (note: the signals shown here are collected from sensor 1 with PLB along OA direction at point 1, refer Figure 2). The wave peaks above threshold level and wave propagation time are minimised with the addition of coating compared to bare pipelines. An observation reveals that both coated pipelines exhibit lower wave peaks and quicker decay time of wave compared to the bare pipeline due to the damping behaviour of coating. An increased damping rate on the pipeline surface cause a decrease in the AE waves parameters [38].

The number of wave peaks directly depends on the materials properties of Young's modulus, density and shape [8,9]. Bare titanium shows the high AE counts above the threshold level compared to the mild steel pipeline due to high thickness and low density. High thickness of the pipeline provides the enough space for the wave propagation and increases the decay time. In both pipelines (coated conditions), the AE counts are reduced with a decrease in the decay time due to the damping behaviour of the epoxy phenolic coating layer compared to the bare conditions of mild steel and titanium pipelines, as shown in Figure 7(a,d). Particularly, the significant gap between the bare and coated conditions of AE counts demonstrates the effect of coating. The pipeline and coating properties influence AE wave peaks and the wave decay time. The PLB test was applied on the coating surface, and a high number of transmitted waves moving from the coating to the pipelines due to the low density and elastic modulus of the coating provided the high velocity of the waves. The transmitted waves from the pipeline to the coating are low because of the pipeline's thickness and high density compared to the

coating, reducing the wave's velocity [39]. Figure 7(b,c,e,f) illustrates the changes in AE parameters, specifically peak amplitude and wave duration, in both bare and coated pipelines. Analysing peak amplitude changes is crucial to confirming the coating's impact on AE waves. Coated pipelines exhibited minimised peak amplitudes compared to bare pipelines, indicating the influence of the coating layer. Furthermore, peak amplitude is highly dependent on incident waves rather than those reflected or transmitted from the pipeline boundary. As seen in the time domain analysis, the wave propagation duration time reduced in the coated conditions of both pipelines, attributed to the damping behaviour of the coating layer, resulting in rapid wave diffusion.

Figure 8 displays the frequency domain analysis of mild steel and titanium pipelines under both bare and coated conditions. The wave velocity correlates directly with frequency and thickness of the material, and the recorded frequency is highly dependent on the frequency range of the sensor [40]. The bare mild steel pipeline has a prominent frequency peak at 50 kHz, with low power spectral density (PSD) peaks visible between 150 kHz and 400 kHz. In contrast, the coated mild steel pipeline shows a peak at 50 kHz, followed by a very low-level negotiable peak. The bare titanium pipeline has a high-level frequency maximum peak at 320 kHz, along with a dominant peak at 50 kHz and small peaks across the range of 100–250 kHz. The high wave frequency and thickness of the pipeline contribute to improved wave velocity on the titanium pipeline. Conversely, coated titanium pipeline reveals a high peak at 50 kHz and a small peak at 320 kHz, with a decrease in power density under coated conditions. Coated pipeline frequency peaks are in the low-frequency range, displaying lower power density at 320 kHz due to different velocity mediums of the pipeline and coating. Multiple frequency peaks are observed in bare pipeline conditions, and these reduce in coated pipelines. The coating layer reduces wave velocity and significantly decreases decay time of waves, resulting in low-frequency peaks with lower power density. The high range of the frequency changes happens between the bare and coated pipeline because the layer of coating (introducing damping) with its density, elastic modulus changes on pipeline surface control wave's velocity.

Figure 9(a,d) shows wave pattern of bare mild steel and titanium pipelines. The signals clearly indicate that high-frequency, low-amplitude wave arrives first and followed by low-frequency, high-amplitude wave on both pipelines, as highlighted in Figure 9(a,d). From the dispersion curves presented in Figure 5, it can be seen that the high-frequency S0 arrives first at the sensor followed by other waves. From the WT plots, it can be seen that first arrival in both the pipes is S0 and A0 followed by other wave modes. It is interesting to note that the largest amplitude is associated with the low-frequency A0 in the mild steel pipe, whereas the highest amplitude is associated with the high-frequency (300–400 kHz). However, it was not possible to determine which wave mode this is associated with in this analysis. Understanding the arrival sequence and behaviour of wave is crucial for analysing integrity and surface conditions of pipeline. The WT of a signal collected from the mild steel pipeline bare and coated conditions, along with the superimposed dispersion curves, is presented in Figure 9(b,c) It is important to note that significant changes in wall thickness have a considerable impact on the dispersion curve. In these experimental conditions, the wall thickness was increased at a micrometre level (about 272 μm on mild steel pipeline, and 306 μm on titanium

Table 2. Representation of wave velocity of bare and coated pipelines.

		Wave velocity (m/s)	
Sr. no.	Pipeline sample	Bare	Coated
1	Mild steel	5357	4934
2	Titanium	5681	5357

pipeline) in coated conditions. The micrometre thickness changes make very minimal wave frequency change from the first order, which is negligible for the dispersion curve measurement. As a reason, only the pipeline thickness (i.e. 5 mm thickness for mild steel pipeline, and 18 mm thickness for titanium alloy pipeline) dispersion curve was applied here. The same frequency window (i.e. from 0–450 kHz) was applied in all the experimental conditions to find the energy zone changes based on the wall thickness and surface conditions. From visual observations, for bare mild steel, high energy zones are in the low-frequency range close to 50 kHz. The wave's amplitude is low in the 150–300 kHz range until the full wave's decay due to the high density of the pipeline. WT indicates that symmetrical waves arrived first at the sensor, followed by the anti-symmetrical waves. In coated conditions, amplitude peaks are lower in the same frequency range, and coating significantly affects AE wave propagation because two different medium layers carry AE waves. The symmetric and antisymmetric wave amplitude levels decreased in the coated pipeline with respect to the same frequency range corresponding to bare pipeline. The second level of the symmetric waves (S1) shows a very low amplitude of close to 300 kHz under both conditions. The study confirms the influence of coating on the pipeline surface on AE waves propagation and amplitude.

The WT of signals collected from titanium pipeline in bare and coated conditions, along with the dispersion curves, is shown in Figure 9(e,f). Visual observation shows multiple energy zones over the frequency range in the bare titanium pipeline compared to two higher energy zones in the coated titanium pipeline, resulting in an overall lower energy level in coated conditions. The titanium pipeline provides high velocity for waves and shows many energy zones over the wave's diffusion time. The S0 and A0 waves propagate with a moderate amplitude in the frequency range of 50–400 kHz. The reflected symmetric and antisymmetric waves show a mixed amplitude level from 100 kHz to 400 kHz frequency level in bare conditions. In the coated pipeline, the amplitude levels of reflected S0 and A0 waves are slightly reduced at the frequency level of 100–400 kHz due to the coating conditions resisting wave propagation and different layer properties affecting the velocity of the wave. In coated conditions, the amplitude level of the wave relates to the density and elastic modulus of the pipeline and coating layers. The remaining PLB test directions of OB, PA, PB, AC, BC and IA, IB showed similar time and frequency domain signals and WT as the direction of OA on bare and coated mild steel and titanium pipelines.

The wave velocity (calculated using $v = \frac{\Delta d}{\Delta t}$) [41] in bare and coated pipeline conditions has been presented in Table 2, where the gap between two sensors is taken as distance (Δd), and the arrival time difference (Δt) is the wave received at sensor 1 and sensor 2. The wave velocity analysis was utilised to find the velocity changes with pipeline

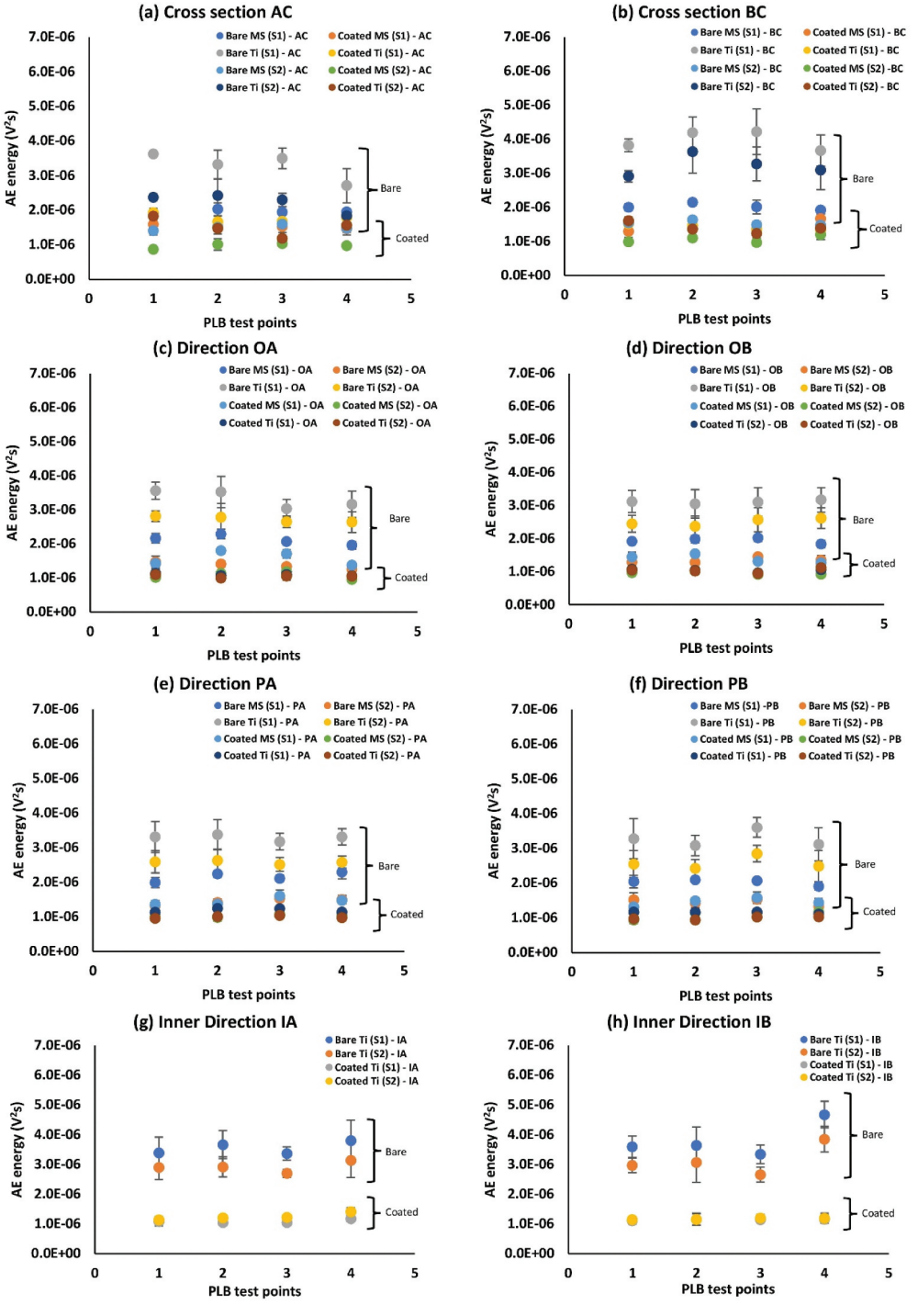

Figure 10. PLB tests AE energy analysis (bare and coated pipelines (mild steel and titanium)): (a) cross section AC, (b) cross section BC, (c) direction OA, (d) direction OB, (e) direction PA, (f) direction PB, (g) inner direction IA and (h) inner direction IB.

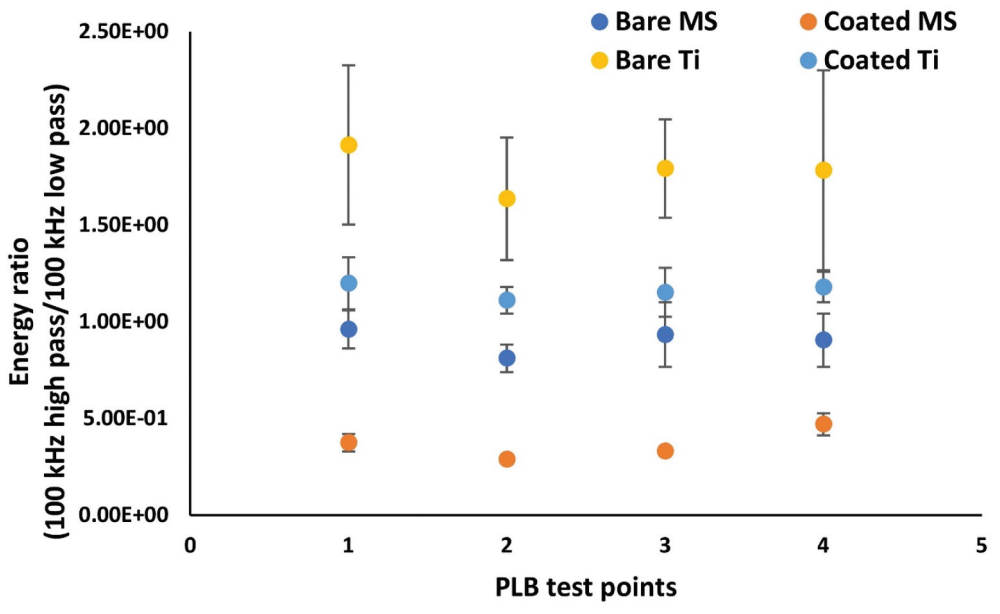

Figure 11. Energy ratio comparison between bare and coated pipelines (mild steel and titanium).

surface conditions. It was observed that the wave velocity of the coated pipeline is reduced compared to the bare condition on both pipelines.

The energy levels of coated mild steel and titanium pipelines are lower compared to bare mild steel and titanium pipelines on sensors 1 and 2 due to the damping effect of the coating layer on the pipeline surface. In coated conditions, waves start from a PLB test point on the coating layer, travel through the coating to the pipeline and reflected waves travel back from the interface and transmitted waves enter pipeline. In this way, propagation happens continuously until complete wave decay, and the sensor on the coating layer collects waves based on reflected and transmitted waves travelling on the coating and pipeline mediums. The two different density mediums impact the movement of waves, reduce waves' strength and enhance wave decay, resulting in energy loss. Compared to bare conditions, coated titanium pipeline exhibits high energy loss due to its thickness, density and elastic modulus difference between pipeline and coating, leading to a quick decay time for waves. Additionally, the smaller thickness of the coating enhances the decay time of the waves [39]. Compared to a bare pipeline, the coated mild steel energy level is slightly low. The standard deviation range is low for the coated conditions, possibly due to the damping behaviour of the coating layer, minimising energy variation in repeated experiments. The energy level of PLB tests on the inner surface (on bare surface) clearly distinguishes between the bare and coated conditions. Energy comparisons for all PLB test points are shown in Figure 10, showing a similar low energy behaviour in coated conditions of mild steel and titanium pipelines.

It is well known that wave velocity is inversely proportional to the density (ρ) of the material [42]. Additionally, the transmission of waves through an interface depends on the interface conditions. Coating delamination and third particles at the interface directly reduce wave velocity [43]. Similarly, as demonstrated through this

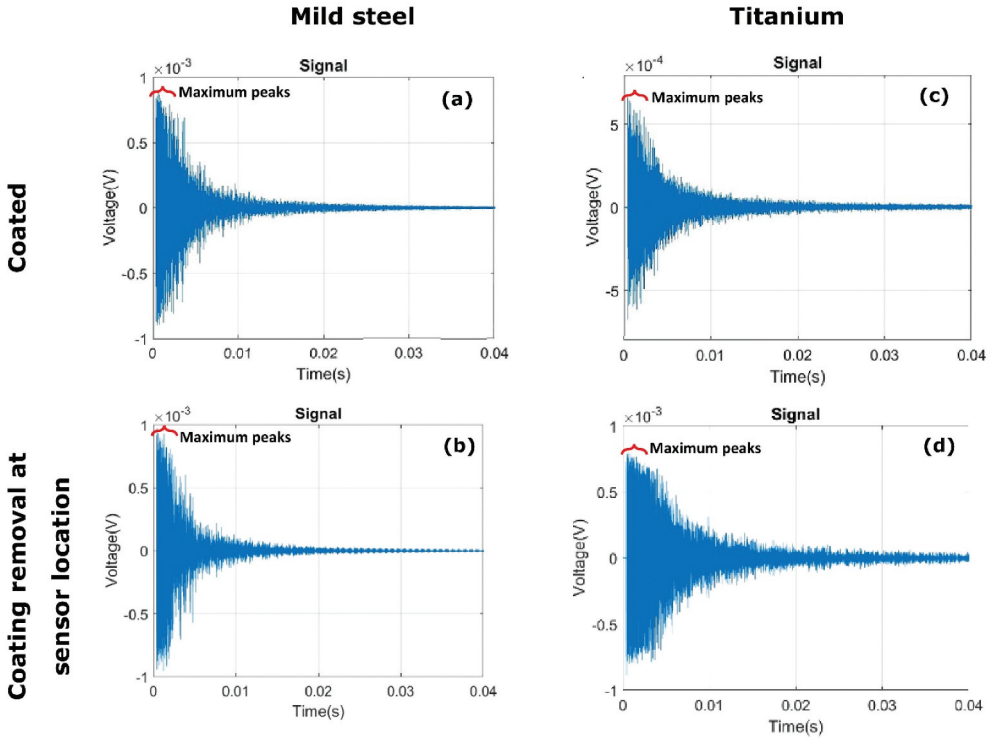

Figure 12. Representative examples of time domain signals: mild steel: (a) coated (b) coating removal, titanium: (c) coated and (d) coating removal.

work, the propagation behaviour of waves depends on the difference in material properties between the base material (pipeline) and coating. It was observed that wave velocity, AE counts, wave decay time and energy levels (section above) are reduced in the coated conditions compared to bare conditions of mild steel and titanium pipelines due to the primary effect of the damping behaviour of the coating on the pipeline.

Figure 11 presents a comparison of the energy ratio (i.e. energy ratio = 100 kHz high pass/100 kHz low pass) between bare and coated pipelines. The energy ratio is decreased in the coated conditions due to absorption of the high frequencies, resulting in low energy in above 100 kHz. The continuous wave transmission in the pipeline and coating is disturbed by the changes in the properties of the two wave propagation mediums, leading to high transmitted waves. Furthermore, the wall thickness of the layer (coating and pipeline) is connected to the wave velocity. A high wall thickness of the pipeline provides sufficient space for the wave's propagation, increases the decay time of waves and shows better wave velocity [39]. The thin coating thickness (in this case epoxy phenolic coating on mild steel and titanium pipeline) is a dominant factor causing low wave velocity in coated pipelines. If necessary, selecting coating materials with properties close to a base material (pipeline), and a coating wall thickness close to that of the base material (pipeline) could help in evaluating the wave transmission and establish this hypothesis further.

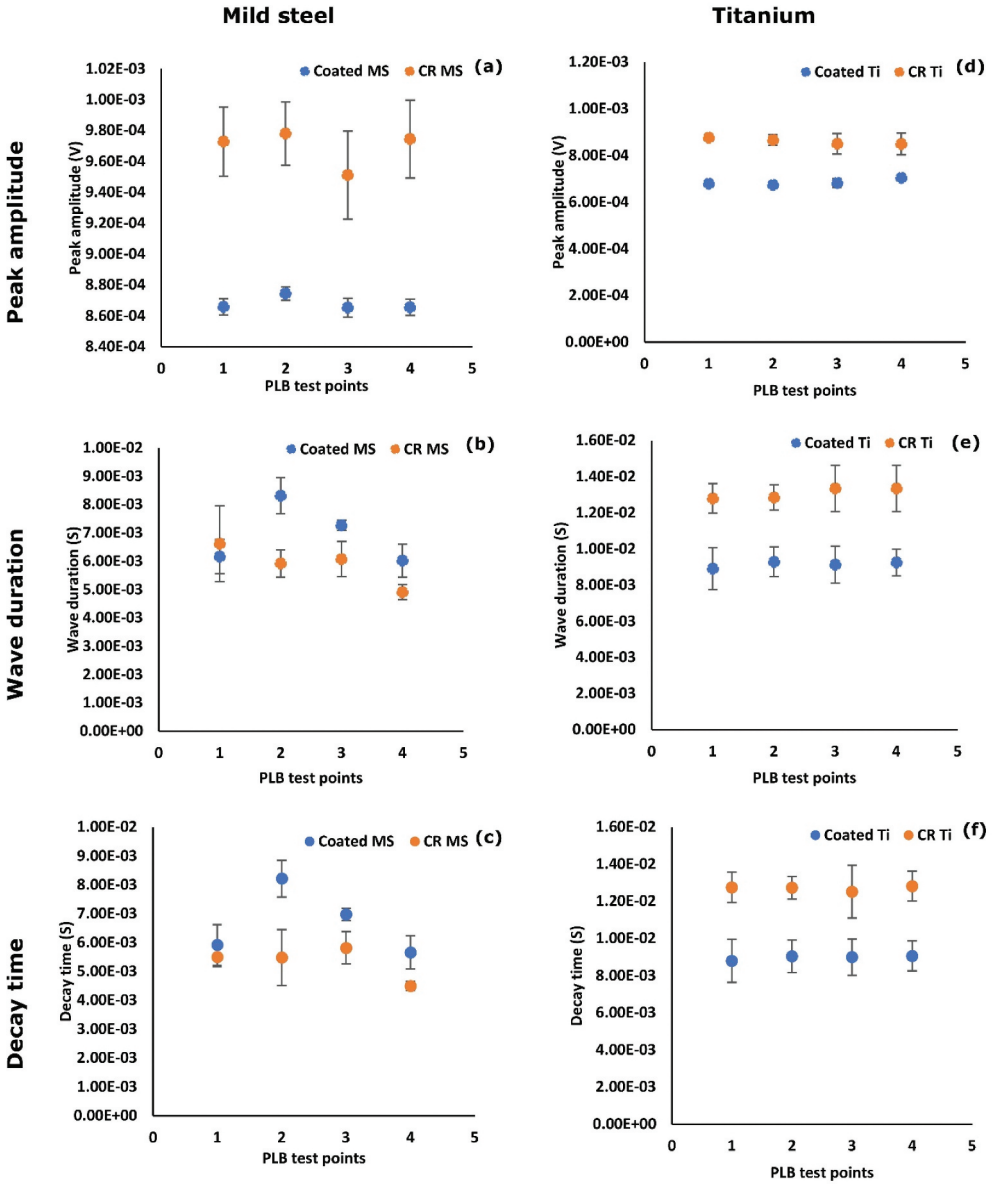

Figure 13. AE parameters comparison, mild steel: (a) peak amplitude, (b) wave duration, (c) decay time; titanium: (d) peak amplitude, (e) wave duration and (f) decay time.

3.2. *Analysis of the effect of sensor location*

Figure 12 presents the AE wave signatures for pipelines with coating and CR at sensor locations. The presence of maximum sharp peaks at the beginning indicates external forces applied on the coating layer (though valid for any AE source, and not specific to coatings). Subsequently, the wave's peak amplitudes decrease over time, and such pattern of peak suggests that the coating and thickness of coating influence the wave's oscillation behaviour [44]. Particularly, mild steel and titanium pipelines show their unique

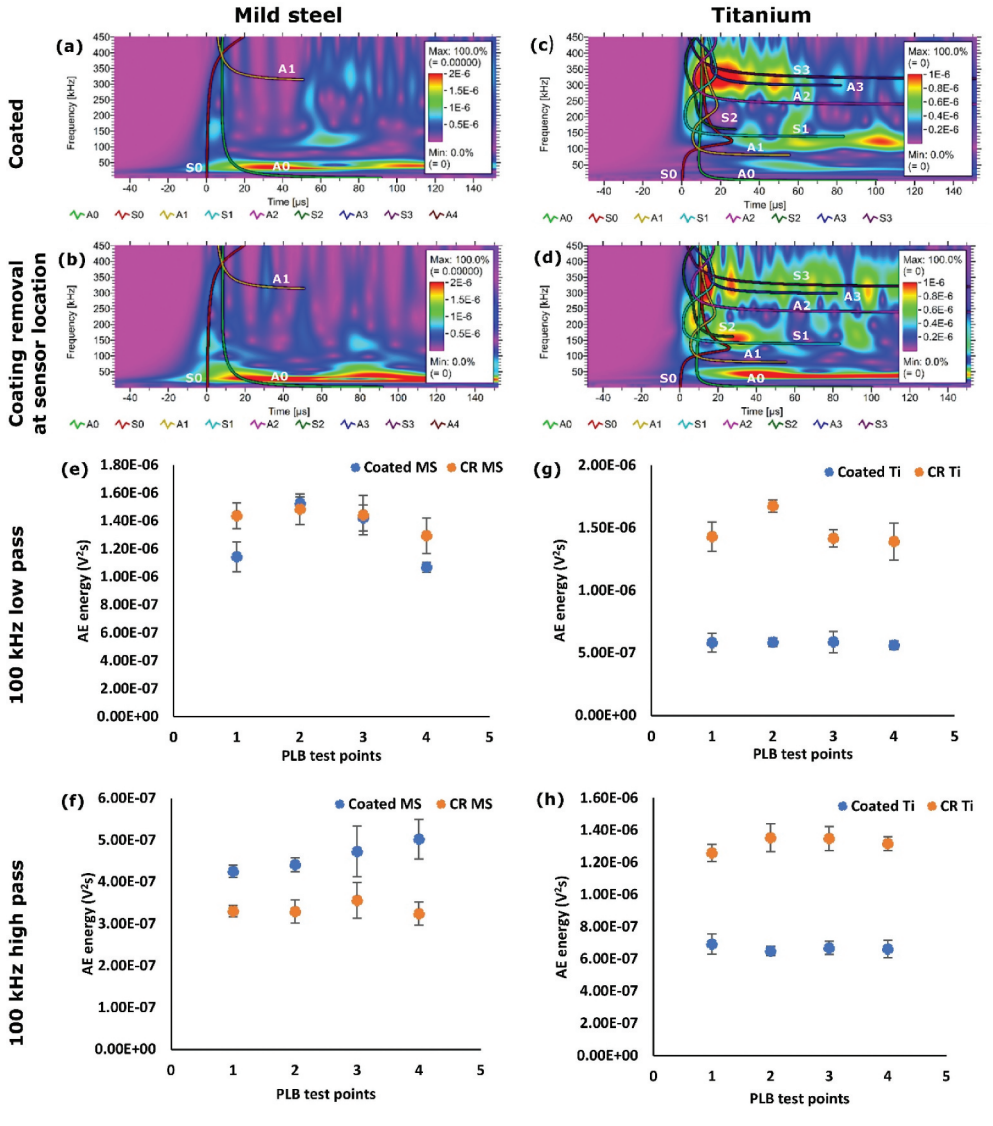

Figure 14. Representation of wavelet transform: (a) coated mild steel, (b) coating removal mild steel, (c) coated titanium and (d) coating removal titanium, and energy level comparison mild steel: (e) 100 kHz low pass, (f) 100 kHz high pass, titanium: (g) 100 kHz low pass, (h) 100 kHz high pass.

behaviour in the time domain analysis. Visual observations reveal reduced wave propagation in mild steel and increased wave propagation in titanium when the sensor placement directly on the pipeline surface. The direct sensor placed on the pipeline surface gives an advanced way to collecting waves and preventing multilayer wave transmission from reaching the sensor.

AE parameters comparison further confirms the significance of sensor location on monitoring. Figure 13 presents the changes in peak amplitude, wave duration and wave decay time in mild steel and titanium pipelines, comparing the effects of sensor placement on coating and CR at sensor locations. The mild steel pipeline exhibited

increased peak amplitude and minimisation of wave decay time, attributed to the direct sensor placement on the pipeline. This set up allows for quick incident wave collection and avoids wave propagation through the coating to reach the sensor. The coating acts as a barrier, slowing down the wave propagation. Additionally, the absence of waves propagating on the coating could be a reason for the low wave duration time. Notably, the high level of CR mild steel peak amplitude demonstrates a wide range of value changes. In contrast, the titanium pipeline displayed a uniquely increased wave duration and wave decay time with increased peak amplitude in the CR conditions at sensor locations. The increased peak amplitude demonstrates that direct placement of sensor collects the wave effectively. The wave duration time and wave decay time increased in the CR conditions at sensor locations compared to coated conditions, possibly due to the higher thickness of the titanium pipeline supporting wave propagation with more reflection. An, Kim and Sohn [45] have noted that the scattering and discontinuity of wave propagation medium affect wave behaviour. Additionally, the sensor placement directly on the pipeline enhanced wave collection. In the coated conditions, the coating properties influenced the waves, minimising the wave duration time.

Frequency domain analysis reveals that the frequency peak of the mild steel is close to 50 kHz, while titanium shows frequency peaks up to 320 kHz in both experimental conditions. Direct sensor placement on the pipeline surface does not show significantly change the wave frequency level. However, the power density of wave frequencies increases when the sensor is in direct contact with the pipeline compared to the sensor on coating. Figure 14(a-d) presents the WT of coated and CR at sensor locations for mild steel and titanium pipelines with dispersion curves. A high amplitude zone appeared for an initial short time, followed by amplitude leave decreases. In both experimental conditions with the coating layer on the pipeline, the density difference between the coating and pipeline reduces wave velocity. Amplitude is increased in the low frequency during CR conditions, particularly with enhanced energy zones observed in titanium pipeline CR at sensor locations. The S0 and A0 waves show a low amplitude level in the low-frequency range, while the reflected symmetric and anti-symmetric waves show a high amplitude level for an initial short time in the frequency range from 100 kHz to 400 kHz in the sensor on the titanium pipeline condition. Amplitude range increases in the same frequency window in the CR at sensor locations.

The energy level comparison based on the frequency window of two different experimental conditions highlights the significance of sensor location in monitoring, as depicted in Figure 14(e-h). The mild steel pipeline exhibits mixed energy level behaviour in the low frequency range (100 kHz low pass) under both coated and CR conditions. Reduced energy level is observed in the mild steel pipeline during CR conditions, attributed to the mission of monitoring high-frequency waves (100 kHz high pass) propagating on the coating. In contrast, titanium shows an increased energy level in CR conditions in both frequency windows, supported by the sensor placement directly on the titanium pipeline, allowing wave monitoring without restriction from the coating. The high wall thickness of titanium serves as a second reason, minimising wave propagation restrictions and diffusion, resulting in an increased energy level of waves. The PLB test results in the OB, PA, PB, AC, BC, IA and IB directions also show similar time and frequency domain signals and WT.

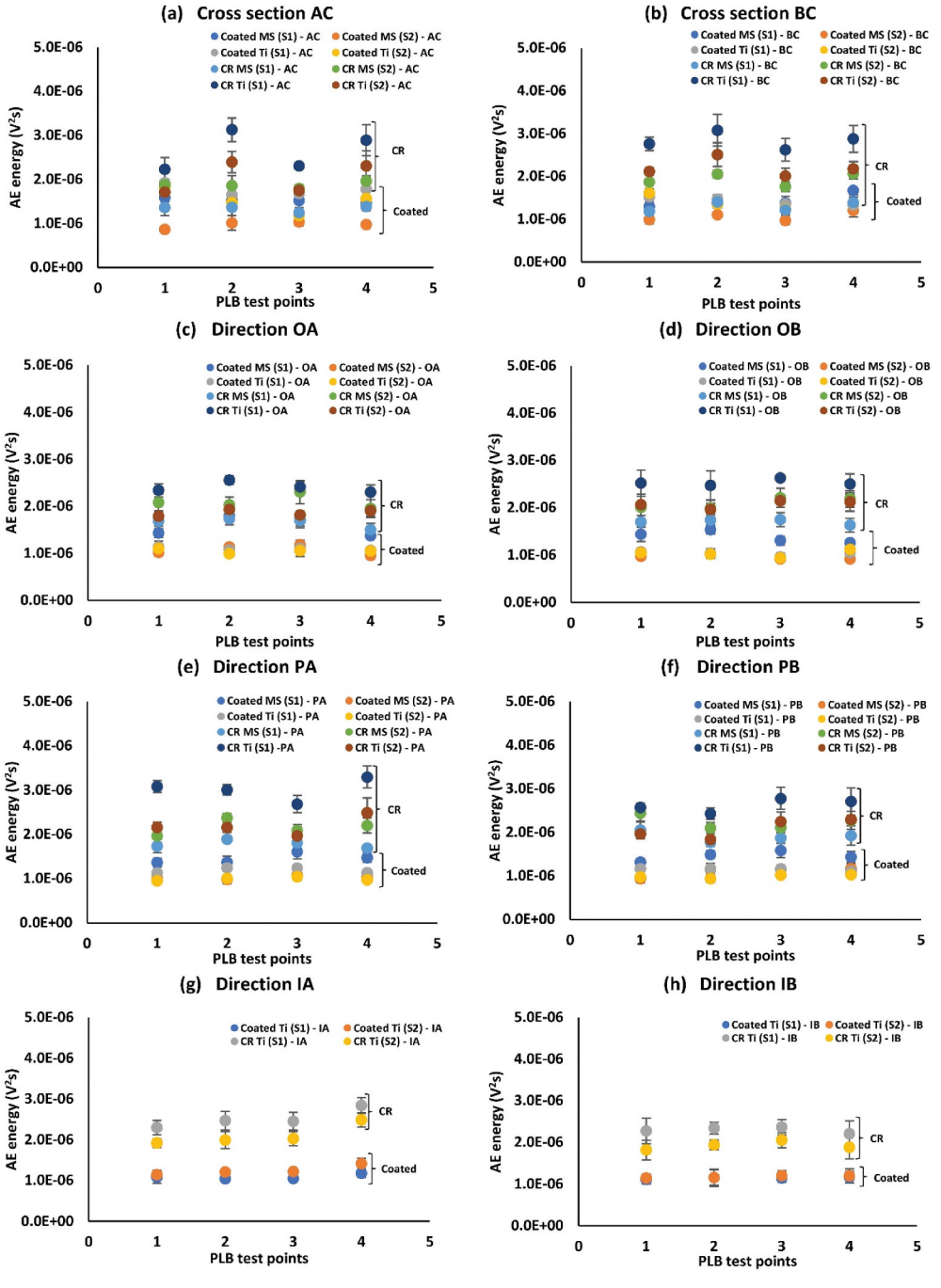

Figure 15. PLB test AE energy analysis (coated and coating removal conditions; mild steel and titanium): (a) cross section AC, (b) cross section BC, (c) direction OA, (d) direction OB, (e) direction PA, (f) direction PB, (g) direction IA and (h) direction IB.

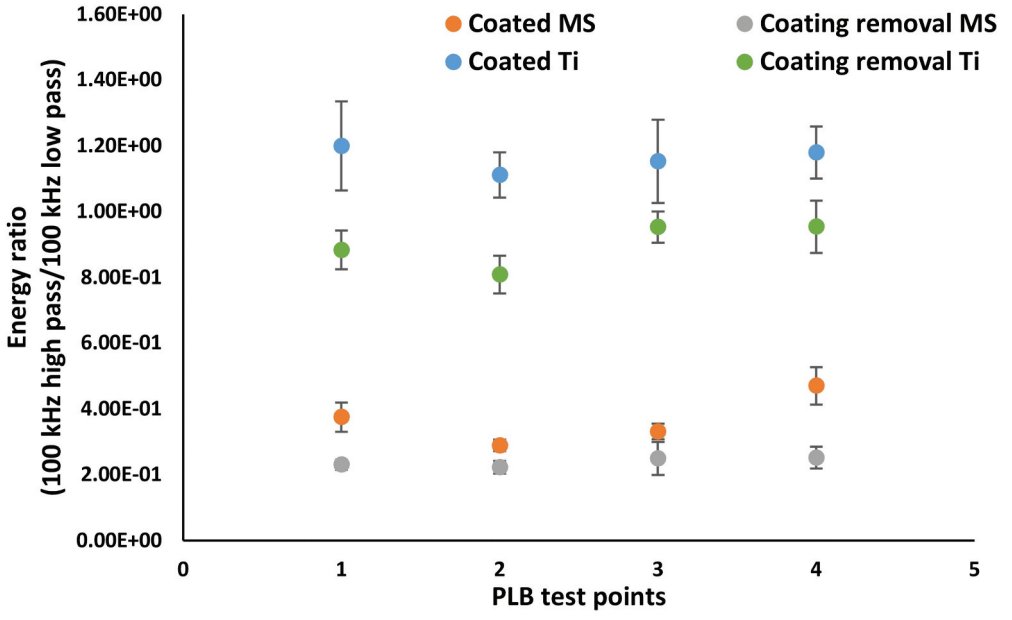

Figure 16. Energy ratio comparison (coated and coating removal conditions; mild steel and titanium).

Figure 15 illustrates AE energy levels (at sensors 1 and 2) with standard deviations for coated and CR at sensor locations for mild steel and titanium. Comparisons between coated and CR conditions at sensor locations show that Sensors 1 and 2 exhibit lower energy levels in coated conditions, while CR typically leads to increased energy levels. The direct mounting of the sensor on the outer pipeline surface in CR conditions allows for swift AE wave collection and avoids the complexities of multilayer wave transmission. Since the pipeline and coating materials have different densities, thicknesses and wave velocities, wave propagation depends on that, and multilayer wave transmission affects the wave's velocity and reflected waves. In coated condition, AE wave transmission happens between the coating and pipeline layers to reach the sensor. A high thickness difference between pipeline and coating enhances wave decay and reduces energy levels. The energy level difference explains and confirms the effectiveness of sensor location on AE monitoring. The direct placement of sensor on pipeline directly monitors AE wave propagation in the pipeline, minimising the impact of coating properties (e.g. density, adherence) on wave collection. Furthermore, the PLB test on the coating (i.e. external pipeline) in both the experimental conditions shows a mixed level of energy behaviour. However, the energy level on the inner surface (i.e. IA, IB direction) provides a clear distinction between the sensor locations on the coating and the direct pipeline surface. In this case, the wave reaches the sensor without the necessity of multilayer wave transmission.

Not much is known about location of AE sensor on coated pipeline and its influence on signals acquired, however, the importance of guided waves and varying directionality has been widely discussed [34]. Strategies regarding sensor location on a two-layer (or multilayer) structure could provide insights into understanding wave propagation

behaviour more effectively. As demonstrated through our work (in this case, epoxy phenolic coated mild steel and titanium pipeline), the location of sensor (on coating, on the pipeline) makes a difference in signals acquired. Figure 16 shows the energy ratio (i.e. energy ratio = 100 kHz high pass/100 kHz low pass) comparison of the two different experimental conditions. It was observed that the energy ratio decreased in the CR conditions. This was due to slight energy level decrease in the high frequencies and dominant energy behaviour on the low frequency below 100 kHz (shown in Figure 14). As a recommendation, for monitoring the primary materials (e.g. pipeline, tank) in the coated conditions, directly placing the sensor on the primary monitoring material surface to get quick and quality data rather than sensor placement on the coating layer surface. This direct sensor placement on primary material surface can prevent associated energy loss. This approach could be beneficial when the primary material has a multilayer condition (e.g. coated pipeline with insulation layers). The sensor placement directly on primary material surface could detect certain changes with the advantage of avoiding the wave scattering and losses in layers to reach the sensor when the sensor is assembled on an outer surface of a multilayer system.

4. Conclusion

This investigation is first-of-a-kind, where a systematic experimental analysis of AE wave propagation in metal pipelines of the same length has been carried out to identify the effects of coatings, pipeline materials (density), pipe wall thicknesses, wave propagation directionality and effect of sensor placement. Wave propagation has been investigated in six pipeline samples: (i) bare mild steel, (ii) bare titanium, (iii) epoxy phenolic coated mild steel, (iv) epoxy phenolic coated titanium, (v) mild steel pipeline epoxy phenolic CR at the sensor location and (vi) titanium pipeline epoxy phenolic CR at the sensor location. All variables play a significant role in the propagation of waves. The recorded signals were analysed for various test conditions using WT to explore time-frequency features to allow the identification of wave modes and assessed the influence of coating layer and sensor location. The following conclusions are drawn from this investigation:

(a) Pipeline wave propagation patterns and AE parameter changes occur due to coated surface conditions of the pipeline compared to bare pipeline. These effects are evident in both time and frequency domains, AE parameters comparison as well as in WT signals, and energy level decreases in both coated pipelines. Particularly, the difference in properties between the coating and pipeline materials results in significant minimisation of high-frequency waves and quick dispersion. However, low-frequency waves are not as greatly affected by these differences. The coating layer showed considerable damping on high-frequency waves.
(b) Based on the results obtained from both the coated and CR at the sensor locations, the significance of sensor location is confirmed with the time and frequency domain and WT signals, along with energy levels. Overall, the wave analysis demonstrates that wave propagation monitoring of coated pipeline could be done effectively with sensors placed on the pipeline surface compared to sensors placed on the coating surface. This can minimise the necessity of wave transmission through coating layer to reach sensor and reduce the effect of coating layer on

wave propagation. However, this is highly dependent on the specific applications and monitoring purposes.

(c) The high wall thickness and low density of the pipeline result in a high number of reflected waves and increased decay time of waves in the titanium pipeline compared to the low wall thickness of mild steel pipeline. Both pipelines showed significant changes in wave propagation in coated conditions compared to bare conditions. The difference in density and thickness between the coating and pipeline hinders wave propagation, affecting wave parameters and wave velocity.

(d) Where possible, while performing PLB tests on internal locations of the pipeline (i.e. bare and coated titanium), it was observed that in the coated pipeline, the energy level is lower than the bare pipeline due to the outer coating layer's damping behaviour on the pipeline where AE waves propagate. The difference in energy level during internal PLB test was observed based on the sensor location in both experimental conditions of titanium pipelines. The results show that the internal pipeline conditions can be monitored through an AE sensor located on the pipeline's outer surface; however, a detailed study is needed to classify the internal pipeline AE sources (defects, cracks) from external pipeline area sources.

This work so far has focused on small length pipeline sections, in which wave propagation was investigated in bare and coated conditions. This investigation is a precursor to further studies where the pipeline could be insulated with an insulation layer operated under various test conditions (e.g. dry, wet, soaked; room temperature, elevated or cryogenic temperatures; with and without coatings; with and without defects in coatings or at the interface), and potentially associate AE generated due to electrochemical activities or degradation at the interface. As this work progresses towards further testing for CUI and in buried pipeline applications, the methodology presented in this research will begin to play an important part in novel detection and characterisation of interface regions by AE technique [46–49].

Nomenclature

Variables

Δd	Distance between sensors
Δt	Time difference
A	Antisymmetric wave
C_g	Group velocity (m/ms)
C_p	Phase velocity (m/ms)
M	Elastic modulus (Pa)
S	Symmetric wave
t	Time
v	Wave velocity (m/s)
V	Voltage
ρ	Density (kg/m^3)

Abbreviations

AE	Acoustic emission
ASTM	American Society for Testing and Materials
CR	Coating removal
CUI	Corrosion under insulation

L	Length (pipeline)
mm	Millimetre
MS	Mild steel
MS/s	Million samples per second
NI	National Instrument
OD	Outer diameter
PAC	Physical Acoustics Corporation
PEC	Pulsed eddy current
PLB	Pencil lead break
PSD	Power spectral density
PZT	Lead zirconate titanate
T	Thickness (pipeline wall)
Ti	Titanium
WT	Wavelet transform

Acknowledgments

This research was carried out by the lead author as part of PhD studentship provided by the School of Engineering. We also acknowledge critical, constructive and impartial feedback by corrosion specialists and sensor experts at UK-based company (CorrosionRADAR Ltd).

Disclosure statement

No potential conflict of interest was reported by the author(s).

ORCID

Nadimul Faisal http://orcid.org/0000-0001-5033-6336

Authors' contributions

All authors contributed to the study conception and design of experiments. Material preparation, measurement, data collection and analysis were performed by Vinooth Rajendran. The first draft of the manuscript was written by Vinooth Rajendran, and all authors commented on previous versions of the manuscript. Experimental support was provided by Anil Prathuru and Carlos Fernandez. Conceptualisation, supervision, review and editing were done by Nadimul Faisal, Anil Prathuru and Carlos Fernandez. All authors read and approved the final manuscript.

Statements and declarations

The authors declare that they have no known competing financial interests or personal relationships that could have appeared to influence the work reported in this paper.

References

[1] Eltai EO, Musharavati F, Mahdi ES. Severity of corrosion under insulation (CUI) to structures and strategies to detect it. Corros Rev. 2019;37(6):553–564. doi: 10.1515/corrrev-2018-0102.

[2] Lai S, Chen DY, Chen H, et al. Pulsed eddy current testing of inner wall flaws in pipe under insulation. Procedia Eng. 2015;130:1658–1664. doi: 10.1016/j.proeng.2015.12.334.
[3] Ulapane N, Alempijevic A, Vidal Calleja T, et al. Pulsed eddy current sensing for critical pipe condition assessment. Sensors. 2017;17(10):2208. doi: 10.3390/s17102208.
[4] de Vogelaere F. Corrosion under insulation. Process Saf Prog. 2009;28(1):30–35. doi: 10.1002/prs.10276.
[5] Cho H, Tamura Y, Matsuo T. Monitoring of corrosion under insulations by acoustic emission and humidity measurement. J Nondestruct Eval. 2011;30(2):59–63. doi: 10.1007/s10921-011-0090-z.
[6] Tscheliesnig P, Lackner G, Jagenbrein A. Corrosion detection by means of acoustic emission (AE) monitoring. In: Proceedings of the 19th World Conference on Non-Destructive Testing (WCNDT 2016), Munich, German; 2016 June. p. 13–17.
[7] Shehadeh M, Steel JA, Reuben RL. Acoustic emission source location for steel pipe and pipeline applications: the role of arrival time estimation. Proc Inst Mech Eng Part E J Process Mech Eng. 2006;220(2):121–133. doi: 10.1243/095440806X78829.
[8] Wu Y, Perrin M, Pastor ML, et al. On the determination of acoustic emission wave propagation velocity in composite sandwich structures. Compos Struct. 2021;259:113231. doi: 10.1016/j.compstruct.2020.113231.
[9] Ozevin D, Harding J. Novel leak localization in pressurized pipeline networks using acoustic emission and geometric connectivity. Int J Press Vessels Pip. 2012;92:63–69. doi: 10.1016/j.ijpvp.2012.01.001.
[10] Quy TB, Kim JM. Crack detection and localization in a fluid pipeline based on acoustic emission signals. Mech Syst Signal Process. 2021;150:107254. doi: 10.1016/j.ymssp.2020.107254.
[11] Cole PT, Watson JR. Acoustic emission for corrosion detection. AMR. 2006;13-14:231–236. doi: 10.4028/www.scientific.net/AMR.13-14.231.
[12] Mostafapour A, Davoudi S. Analysis of leakage in high pressure pipe using acoustic emission method. Appl Acoust. 2013;74(3):335–342. doi: 10.1016/j.apacoust.2012.07.012.
[13] Xu C, du S, Gong P, et al. An improved method for pipeline leakage localization with a single sensor based on modal acoustic emission and empirical mode decomposition with Hilbert transform. IEEE Sensors J. 2020;20(10):5480–5491. doi: 10.1109/JSEN.2020.2971854.
[14] Barat V, Terentyev D, Bardakov V, et al. Analytical modeling of acoustic emission signals in thin-walled objects. Appl Sci. 2019;10(1):279. doi: 10.3390/app10010279.
[15] Su Z, Ye L. Identification of damage using lamb waves: from fundamentals to applications. Vol. 48. Springer Science & Business Media; 2009. doi: 10.1007/978-1-84882-784-4.
[16] Mahmoud H, Mazal P, Vlasic F. Relationship between acoustic emission signal and loads on pneumatic cylinders. Nondestr Test Eval. 2020;35(2):222–238. doi: 10.1080/10589759.2019.1662900.
[17] Jones MR, Rogers TJ, Worden K, et al. A Bayesian methodology for localising acoustic emission sources in complex structures. Mech Syst Signal Process. 2022;163:108143. doi: 10.1016/j.ymssp.2021.108143.
[18] Świt G, Dzioba I, Adamczak-Bugno A, et al. Identification of the fracture process in gas pipeline steel based on the analysis of AE signals. Materials. 2022;15(7):2659. doi: 10.3390/ma15072659.
[19] Świt G, Dzioba I, Ulewicz M, et al. Experimental-numerical analysis of the fracture process in smooth and notched V specimens. Produ Eng Archives. 2023;29(4):444–451. doi: 10.30657/pea.2023.29.49.
[20] Świt G, Ulewicz M, Pała R, et al. Innovative acoustic emission method for monitoring the quality and integrity of ferritic steel gas pipelines. Produ Eng Archives. 2024;30(2):233–240. doi: 10.30657/pea.2024.30.22.
[21] Crawford A, Droubi MG, Faisal NH. Analysis of acoustic emission propagation in metal-to-metal adhesively bonded joints. J Nondestruct Eval. 2018;37(2):1–19. doi: 10.1007/s10921-018-0488-y.

[22] ASTM: E 976–99 Standard Guide for Determining the Reproducibility of Acoustic Emission Sensor Response
[23] Falcetelli F, Romero MB, Pant S, et al. Modelling of pencil-lead break acoustic emission sources using the time reversal technique. In: Proceedings of the 9th European Workshop on Structural Health Monitoring; Manchester, (UK); 2018 July. p. 10–13.
[24] Sause MG.Investigation of pencil-lead breaks as acoustic emission sources. 2011.
[25] Materials. ASTM A106 properties. [online]. 2020. Available from: https://materials.gelsonluz.com/2020/09/astm-a106-properties-chem-mech-rankings.html
[26] Veiga C, Davim JP, Loureiro AJR. Properties and applications of titanium alloys: a brief review. Rev Adv Mater Sci. 2012;32(2):133–148.
[27] Guven S, Aguloglu S, Beydemir K, et al. Examination of stress distribution and fracture resistance in five-unit tooth-and implant-supported partial fixed zirconia prosthesis. Biotechnol Equip. 2015;29(6):1176–1183. doi: 10.1080/13102818.2015.1073122.
[28] Krishna LSR, Anand BK, Rajan R, et al. Finite element analysis of a fractured mandible fixed with micro plates. Int J Eng Sci Tech. 2017;9(7): 784–795.
[29] Dixit D, Pal R, Kapoor G, et al. Lightweight composite materials processing. In: Lightweight ballistic composites. Woodhead Publishing; 2016. p. 157–216. doi: 10.1016/B978-0-08-100406-7.00006-4.
[30] Lane R, Hayes SA, Jones FR. Modelling the effect of a discrete interphase on the fragmentation process in polymer matrix composites. ICCM-12: 12th International Conference on Composite Materials; 1999 July 5–9; Paris. 2014. https://iccm-central.org/Proceedings/ICCM12proceedings/papers/pap281.pdf.
[31] Faisal NH, Ahmed R. Acoustic emission analysis of Vickers indentation fracture of cermet and ceramic coatings. Meas Sci Technol. 2011;22(12):125704. doi: 10.1088/0957-0233/22/12/125704.
[32] El-Sherik AM, editor. Trends in oil and gas corrosion research and technologies: Production and transmission. Duxford, UK: Woodhead Publishing; 2017.
[33] Barroso-Romero M, Gagar D, Pant S, et al. Wave mode identification of acoustic emission signals using phase analysis. Acoustics. 2019 June;1(2):450–472. doi: 10.3390/acoustics1020026.
[34] Fromme P. Guided wave testing. Springer; 2018. doi: 10.1007/978-3-319-30050-4_24-1.
[35] Gupta A, Duke JC Jr. Identifying the arrival of extensional and flexural wave modes using wavelet decomposition of ultrasonic signals. Ultrasonics. 2018;82:261–271. doi: 10.1016/j.ultras.2017.09.008.
[36] Boller C, Chang FK, Fujino Y. Encyclopedia of structural health monitoring. New York: John Wiley & Sons; 2009. doi: 10.1002/9780470061626.
[37] Droubi MG, Reuben RL, White G. Statistical distribution models for monitoring acoustic emission (AE) energy of abrasive particle impacts on carbon steel. Mech Syst Signal Process. 2012;30:356–372. doi: 10.1016/j.ymssp.2011.12.017.
[38] Tönshoff HK, Jung M, Männel S, et al. Using acoustic emission signals for monitoring of production processes. Ultrasonics. 2000;37(10):681–686. doi: 10.1016/S0041-624X(00)00026-3.
[39] Maksuti E, Bini F, Fiorentini S, et al. Influence of wall thickness and diameter on arterial shear wave elastography: a phantom and finite element study. Phys Med Biol. 2017;62(7):2694. doi: 10.1088/1361-6560/aa591d.
[40] Mustapha S, Ye L. Non-destructive evaluation (NDE) of composites: assessing debonding in sandwich panels using guided waves. In: Non-Destructive Evaluation (NDE) of Polymer Matrix Composites. Woodhead Publishing; 2013. p. 238–278. doi: 10.1533/9780857093554.2.238.
[41] Wilkening F. Integrating velocity, time, and distance information: A developmental study. Cogn Psychol. 1981;13(2):231–247. doi: 10.1016/0010-0285(81)90009-8.
[42] Bourbié T, Coussy O, Zinszner B. Acoustics of porous media. Editions Technip; 1987.
[43] Tell F, Svensson T. Stress Wave Propagation between-Different Materials [master's thesis]. Sweden: Chalmers University of Technology; 2015. https://www.msb.se/siteassets/doku

ment/amnesomraden/krisberedskap-och-civilt-forsvar/befolkningsskydd/skyddsrum/examensarbeten/l04-112_stress-wave-propagation-between-different-materials.pdf .
[44] Zhao K, Yang D, Gong C, et al. Evaluation of internal microcrack evolution in red sandstone based on time–frequency domain characteristics of acoustic emission signals. Construct Building Mater. 2020;260:120435. doi: 10.1016/j.conbuildmat.2020.120435.
[45] An YK, Kim M, Sohn H. Piezoelectric transducers for assessing and monitoring civil infrastructures. In: Sensor Technologies for Civil Infrastructures. Woodhead Publishing; 2014. p. 86–120. doi: 10.1533/9780857099136.86.
[46] AGU Vallen Wavelet. https://www.vallen.de/products/software
[47] Barile C, Casavola C, Pappalettera G. Acoustic emission waveform analysis in CFRP under Mode I test. Eng Fract Mech. 2019;210:408–413. doi: 10.1016/j.engfracmech.2018.01.023.
[48] Dahmene F, Yaacoubi S, El Mountassir M, et al. On the modal acoustic emission testing of composite structure. Compos Struct. 2016;140:446–452. doi: 10.1016/j.compstruct.2016.01.003.
[49] Droubi MG, Stuart A, Mowat J, et al. Acoustic emission method to study fracture (Mode-I, II) and residual strength characteristics in composite-to-metal and metal-to-metal adhesively bonded joints. J Adhes. 2018;94(5):347–386. doi: 10.1080/00218464.2017.1278696.